Principal Hue Curves and Color Difference

Tarow Indow

Department of Cognitive Sciences, University of California Irvine, Irvine, California 92697

Received 8 August 1998; accepted 7 January 1999

*Abstract: The size of perceptual difference of colors (*j, k*) is scaled as* d_{jk} *by selecting a pair of Munsell grays in which the lightness difference matches in size with the color difference. Hence,* d *is given in terms of Munsell V. The degree of principal hue component* α *in a color* j *is scaled as* ξ_α(j) *by making marks on a line segment and the range of* ξ_α *is from 0 to 10. By plotting* ξ_α*(H V/C) on Munsell H-circle, principal hue curves* $\bar{\xi}_\alpha$*(H V/C) are defined, where* α *= R, Y, G, B, V = 4–7, and C = 2–10. In this process, similar plots of NCS codes* ($c\phi_\alpha$) *are used as references. The curves* $\bar{\xi}_\alpha$*(H V/C) tell us the appearance of Munsell colors (H V/C) and also enable us to predict color differences. The relationship between* d_{jk} *and* $\Delta V = |V_j - V_k|$, $\Delta\bar{\xi}_\alpha = |\bar{\xi}_\alpha(H_j\ V_j/C_j) - \bar{\xi}_\alpha(H_k\ V_k/C_k)|$ *is tested in various ways, e.g., logarithmic, power, Minkowski-type functions. The best predictor* $\tilde{d}$ *is given by a simple linear form,* $\tilde{d} = a_V\Delta V + \{d_0 + \Sigma a_\alpha\Delta\bar{\xi}_\alpha\}$*. For 899 pairs (*j, k*), 706 differing in H, C and 193 differing in H, V, C,* $a_V = 0.459$, $d_0 = 0.610$, $a_R = 0.199$, $a_Y = 0.031$, $a_G = 0.098$, $a_B = 0.136$, *and the root-mean-squares of* ($d_{jk} - \tilde{d}_{jk}$) *is 0.338 in the matched V-unit.* © 1999 John Wiley & Sons, Inc. Col Res Appl, 24, 266–279, 1999

Key words: Munsell system; NCS system; color difference; principal hues

INTRODUCTION

Two predictions from the current Munsell System were discussed in the preceding articles Part I[1] and Part II.[2] One was how to predict the size of difference we see between two Munsell chips, and the other was how to predict the degree of redness, yellowness, etc. that we feel in a Munsell chip. Let us denote by δ_{jk} the perceptual difference between ($H_j\ V_j/C_j$) and ($H_k\ V_k/C_k$), and by $\mathcal{H}_\alpha(j)$, the degree of a principal hue α that we see in (H_j, V_j/C_j), where α = R, Y, G, B, or R, Y, G, B, P(purple). Both δ and $\mathcal{H}_\alpha$ are quantity-like perceptions, but cannot be experienced by anyone other than the observer. Hence, these latent variables must be converted through assessments of the observer to quantitative data, i.e., scaled values. What will be predicted are these scaled values. Scaled values of perceptual color differences δ_{jk}, d_{jk}, were related to $\hat{d}_{jk}$, Euclidean distances between P_j and P_k in the current Munsell solid $\{P_j\}$. Vectors representing principal hues α, $\mathbf{f}_\alpha$, were defined in a plane (H, C) of constant V. The direction of $\mathbf{f}_\alpha$ was not necessarily the same with Munsell $5H_\alpha$, which denotes the Hue code for most representative color of α. Scaled values of principal hues, $\mathcal{H}_\alpha(j)$, $\xi_\alpha(j)$, were related to $\hat{\xi}_\alpha(j)$, the coordinates of P_j on $\mathbf{f}_\alpha$.

On the basis of the same datasets, color differences (d_{jk}) and principal hue assessments ($\xi_\alpha(j)$), the following problems will be discussed in the present article. One is to define curves $\bar{\xi}_\alpha$(H|V/C) that represent the change of principal hues α along Hue circles at various levels of V/C. Then, color differences d_{jk} are reduced to differences in the respective principal hue components $\Delta\bar{\xi}_\alpha = |\bar{\xi}_\alpha(H_j|V_j/C_j) - \bar{\xi}_\alpha(H_k|V_k/C_k)|$ and the lightness difference $\Delta V = |V_j - V_k|$.

The following symbols and abbreviations will be used throughout in this article:

j, k: individual colors.
P_j: points representing a color in a system.
(H V/C): Munsell notations of Hue, Value, and Chroma.
N_x: a gray color on the Munsell Value scale.
δ_{jk}: a perceptual color difference between j and k (latent variable).
d_{jk}: the scaled value of δ_{jk} in terms of matched V-unit.
r(V/C): the ratio of perceptual sizes of 1V to 1C in Munsell notation. (V/C) = 2.3.
( ): a matrix.
{ }: a configuration of points or a set of vectors.
α, β, γ: principal hue components, R(red), Y(yellow), G(green), B(blue), P(purple).
$\mathbf{f}_\alpha$: a principal hue vector in a Munsell plane (H,C) of constant V.
$\hat{d}_{jk}$: a Euclidean distance between P_j and P_k in a configuration $\{P_j\}$ with the unit of Munsell C.

$\hat{\bar{d}}$: $\hat{d}$ converted to the unit of d (matched V-unit), $\hat{\bar{d}} = 0.357\,\hat{d}$.
$\hat{\xi}_\alpha(j)$: the coordinate of P_j on $\mathbf{f}_\alpha$ in terms of C.
$\mathcal{H}_\alpha$: the perceived degree of a principal hue (latent variable).
$\zeta(j)$: the chromatic component in a color j, $0 \le \zeta(j) \le 10$.
N(j): the achromatic component in a color j, $N(j) = 10 - \zeta(j)$.
$\hat{V}(j)$: the matched V-level of N(j).
$\xi_\alpha(j)$: an absolute principal hue component, the scaled value of a principal hue $\mathcal{H}_\alpha$ in a color j, $0 \le \xi_\alpha(j) \le \zeta(j)$, $\zeta(j) = \Sigma_\alpha \xi_\alpha(j)$
$\eta_\alpha(j)$: a relative principal hue component, $\eta_\alpha(j) = \xi_\alpha(j)/\zeta(j)$, $0 \le \eta_\alpha(j) \le 1$.
$\tilde{x}(\ )$: the predicted value of x, $x = d, \xi, \eta, \zeta$, the term(s) in ( ) either predictor(s) or parameter(s).
$\bar{x}$(H|V/C): x defined on the H-circle of V/C, $x = \xi, \eta, \zeta$.
$\varphi_\alpha(\lambda)$: chromatic response functions on the equal-energy spectrum. α = R-G, Y-B.
$\varphi_\alpha\{P(\lambda)\}$: chromatic response functions of monochromatic light of intensity P.
(s, c, ϕ): NCS notations of blackness, chromaticness, and position of the NCS hue circle.
Φ_α: absolute principal hue components of NCS, $\Phi_\alpha = (c\phi_\alpha)/1000$, $0 \le \Phi_\alpha \le 10$.
NR: the number of repeated assessments.
NS: the number of observers.
N: the number of assessed colors (easily distinguished from N for a Munsell gray).
MDS: multidimensional scaling.
RMS: the root-mean-squares of a set of discrepancies of prediction.
L.R: Linear-regression.
$\Delta\theta_\alpha$: $\{\theta_\alpha(j) - \theta_\alpha(k)\}$, $\theta = \bar{\xi}$ or $\bar{\eta}$.
$\Gamma(\Delta\theta_\alpha)$: a linear combination of $\Delta\theta_\alpha$.

DATASETS AND FINDINGS IN THE PRECEDING ARTICLES

For obtaining data d_{jk}, pairs of Munsell chips (j, k) were presented, one pair at a time, and the observer was asked to select a Munsell gray pair (N_A, N_X) such that the lightness difference matches in size with the overall perceptual color difference δ_{jk}, [Fig. 1(A)]. In this way, a covert variable δ was converted to the overt variable $|N_A - N_X|$. With each pair (j, k), selecting matched gray pair (N_A, N_X) was repeated N_R times, not in direct succession, with a fixed gray N_A in a different part on the Value Scale. The ground mean of $|V_A - V_X|$ over N_R repetitions and N_S observers was defined as d_{jk}. Namely, color differences were given in terms of matched differences on Munsell Value Scale V ($0 \sim 10$). When j and k are too different, such as saturated red and green, the matching becomes less intuitive and pairs (j, k) were limited within the range that matching was comfortably made by observers, and, hence, $d_{jk} < 3.5$ V. Results of four experiments were synthesized. The observing conditions and the number N of pairs (j, k) and N_R, N_S in the respective experiments are given in Table I in I.[1]

Figure 1(B) shows a procedure to scale as $\xi_\alpha(j)$ the

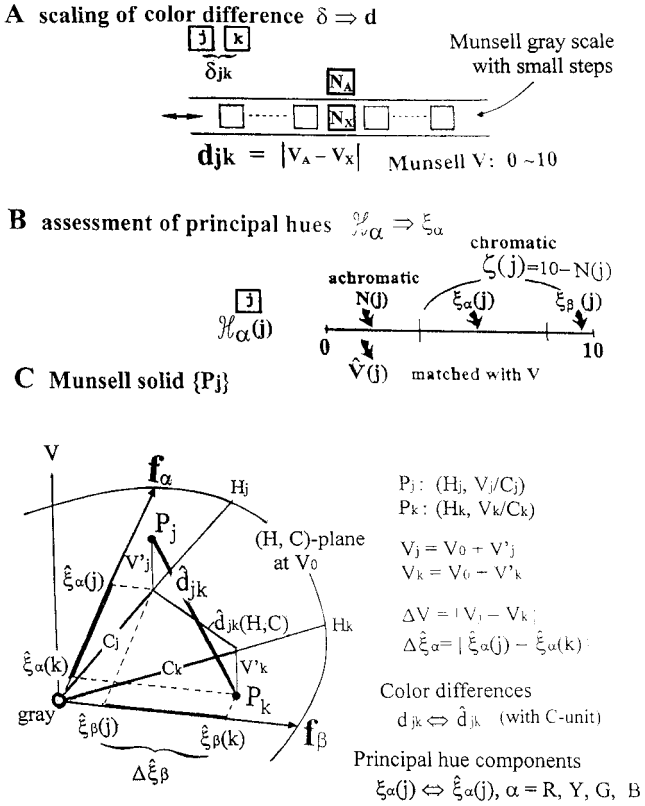

FIG. 1. Procedures to scale color difference δ as d_{jk} and principal hue $\mathcal{H}_\alpha$ as $\xi_\alpha(j)$, and their representations, $\hat{d}_{jk}$ and $\hat{\xi}_\alpha(j)$, in Munsell solid $\{P_j\}$.

degree of a perceptual principal hue component $\mathcal{H}_\alpha$ in a color j. A color j was presented, one at a time, and the observer was asked to make marks on a line segment. First the line was divided into two parts, N(j) and $\zeta(j)$, according to the degrees of achromatic and chromatic impressions felt in this color. Then, the observer made mark(s) in $\zeta(j)$ according to the degrees of principal hues α being perceived in the color. The hue names α to be used were specified in advance, 5 (R, Y, G, B, and P) or 4 (R, Y, G, and B). Usually, the observer made one mark to indicate two principal hue components in $\zeta(j)$, such as R and Y in an orange color j. These lengths were $\xi_R(j)$ and $\xi_Y(j)$. When j was a low-saturated color, sometimes the observer felt it necessary to divide $\zeta(j)$ into three parts. When j was a maximally saturated color of a hue α, no mark was given so that the entire line represented that hue α. Assessments were repeated, not in direct succession, N_R times by N_S observers, and the grand mean was defined as $\xi_\alpha(j)$. The length of line segment was defined to be 10, and, hence, $0 \le \zeta(j) \le 10$, and $0 \le \xi_\alpha(j) \le \zeta(j)$. Results of four experiments were synthesized, and the conditions, the number N of colors j, and N_R, N_S in the respective experiments were shown in Table I in II.[2] Examples of intra-individual standard deviations of N_R repeated assessments and inter-individual standard deviations among N_S observers were shown in Table II in II.[2] In some experiments, the observer was asked to indicate the lightness of achromatic part N(j) by the level of

V on Munsell Value scale. Examples of grand means of matched V, $\hat{V}(j)$, were given in Fig. 2 in II.[2]

In both kinds of experiment, (j, k) or j was presented under the standard light on the gray background. Figure 1(C) shows P_j and P_k representing (H_j V_j/C_j) and (H_k V_j/C_k) in Munsell solid. The Euclidean distance $\hat{d}_{jk}$ is measured with the unit of C. Namely, $\hat{d}_{jk} = 1$ when $H_j = H_k$, $V_j = V_k$ and $C_j = C_k + 1$. A series of multidimensional scaling (MDS) analysis of Munsell solid[3,4] showed it appropriate to decompose d_{jk} into two orthogonal components, $\hat{d}_{jk}$(H, C), the differences in a constant V plane (H, C) and $\Delta V = |V_j - V_k|$, provided the unit of V and the unit of C for $\hat{d}_{jk}$(H, C) are properly equated in terms of perceptual color difference. It is well known that Munsell units for V and C are not perceptually equivalent. According to the MDS studies,[3,4] the most likely value of ratio r(V/C) is 2.3. In Fig. 1(C), (H_j, C_j) and (H_k, C_k) are defined in an arbitrary level of V, V_0. The optimum directions of vectors representing principal hues, $\mathbf{f}_\alpha$, are also defined in this plane. The following findings in I[1] and II[2] are relevant to the subsequent discussion.

1. Scaled value of color difference d_{jk} is proportional to distance $\hat{d}_{jk}$ between P_j and P_k. Define predicted values by $\tilde{d}$, then $\tilde{d}(\hat{d}_{jk}) = (\text{slope})\hat{\hat{d}}_{jk}$, where $\hat{\hat{d}} = 0.357\ \hat{d}$. Namely, $\hat{d}$ is given by the unit of C and $\hat{\hat{d}}$ by the matched V-unit of d. Slopes and root-mean-squares (RMS)'s of discrepancies $[d_{jk} - \tilde{d}(\hat{d}_{jk})]$ were given in Table II in ref. 1. Denote by $\hat{d}_{jk}$(H, C) the distance between P_j and P_k projected to the (H, C) plane. For (j, k) in which $V_j = V_k$ and prediction is $\tilde{d}\{\hat{d}_{jk}(H, C)\}$, and the general level of RMS for these 2-D color differences was 0.3 in term of matched V. For (j, k) in which $V_j \neq V_k$, RMS for $\tilde{d}\{\hat{d}_{jk}(H, C), \Delta V\}$ was about 0.6 V. These levels of accuracy of prediction are better than when predictor $\tilde{d}$ is defined by color difference formulae, such as CIE 1976 ($L^*u^*v^*$), Adams–Nickerson, and modified Judd. When $\tilde{d}$ is defined by CIE 94($L^*C^*H^*$), RMS is slightly smaller. When $\hat{d}_{jk}$ is distance in the configuration constructed by MDS, RMS is 0.2 ~ 0.3 V.
2. Munsell principal hues are 5R, 5Y, 5G, 5B, and 5P. It was shown that Purple is not indispensable in the sense that if P is excluded from α, the ξ_P(H V/C) curve is evenly divided into ξ_R(H V/C) and ξ_B(H V/C).
3. Irrespective of whether P is included or not, $\mathbf{f}_B$ is far shifted from 5B toward 5PB. As to other principal hues α, $\mathbf{f}_\alpha$, are close to the directions of $5H_\alpha$.
4. Data $\xi_\alpha(j)$ are called the absolute principal hue components in a color j, whereas $\eta_\alpha(j) = \xi_\alpha(j)/\zeta(j)$ are called the relative principal hue components. The dynamic range of $\xi_\alpha(j)$ is between 0–10, and that of $\eta_\alpha(j)$ is between 0–1. Data ξ_α(H V/C) are fitted by power functions of $\hat{\xi}_\alpha$(H V/C), coordinates of P(H V/C) on $\mathbf{f}_\alpha$, $\tilde{\xi}_\alpha(H, V/C) = A_\alpha(V, C)\ \hat{\xi}_\alpha(H\ V/C)^{B_\alpha(V,C)}$. The parameters, A_α(V, C) and B_α(V, C), are shown in Fig. 7 in ref. 2. As a matter of course, η_α(H V/C) is more independent of V/C than ξ_α(H, V/C) is. Still, η_α(H V/C) does not remain completely invariant for different levels of V/C. Change due to V is especially marked in yellowish colors.
5. When ξ_α(H V/C) and η_α(H V/C) are plotted on the H-circle at a fixed level of V/C, curves are, respectively, denoted as $\xi_\alpha(H|V/C)$ and $\eta_\alpha(H|V/C)$. Curves $\eta_\alpha(H|V/C)$ at various levels of V and C are shown in Fig. 11 in ref. 2. Curves $\xi_\alpha(H|V/C)$ represent changes of absolute principal hue components α along the H-circle of V/C.

Curves analogous to $\xi_\alpha(H|V/C)$ for monochromatic light of intensity $P(\lambda)$ are defined from the chromatic response functions $\varphi_\alpha(\lambda)$ for equal-energy spectrum $P_0(\lambda)$. Degrees of two opponent processes, R–G and Y–B, in $P_0(\lambda)$, $\varphi_\alpha(\lambda)$, were first formulated by the cancellation method.[5,6] When $P(\lambda) = kP_0(\lambda)$, the degree of a hue α in $P(\lambda)$, $\varphi_\alpha\{P(\lambda)\}$, is defined as $K_\alpha(k)\varphi_\alpha(\lambda)$, and $\varphi_\alpha\{P(\lambda)\}$ tells us the intensity of the complementary light necessary to cancel the hue α when it is additively mixed with $P(\lambda)$. Coefficient $K_\alpha(k)$ is assumed as a linear function of k, and steeper for the process Y–B than the process R–G. Hurvich[7] described how to define φ_α for nonmonochromatic light.

It was emphasized that the predictor $\tilde{d}(j, k)$ or $\tilde{\xi}_\alpha(j)$ does not represent perception δ_{jk} or $\mathcal{H}_\alpha$ *per se*. What is predicted is the observable data scaled in the ways as described above. We cannot say how the observer converts the subjective experience, δ or $\mathcal{H}_\alpha$, to the observable response d or ξ [Fig. 1(A, B)]. The situation is the same with $\varphi_\alpha\{P(\lambda)\}$ for light stimulus. Though we can predict the intensity of the complementary light necessary to cancel the hue α in its appearance, we cannot say how $\varphi_\alpha\{P(\lambda)\}$ is related to the perceptual intensity of hue $\mathcal{H}_\alpha$ that the observer sees in the monochromatic light $P(\lambda)$.

In the previous study Part II,[2] curves $\tilde{\xi}_\alpha(H|V/C)$ were first defined by relating data ξ_α(H, V/C) to $\hat{\xi}_\alpha$(H, V/C), coordinates of P(H V/C) on principal hue vector $\mathbf{f}_\alpha$, α = R, Y, G, B, and R, Y, G, B, P. In the present study, a new set of representative curves $\bar{\xi}_\alpha(H|V/C)$, on H-circles at V/C are formulated directly from data $\xi_\alpha(j)$. Since Purple P was found redundant, only four curves $\bar{\xi}_\alpha(H|V/C)$, α = R, Y, G, B, are considered. Datasets $\xi_Y(j)$ and $\xi_G(j)$ of 4 and 5 hue assessments are, respectively, combined, because these are unrelated to Purple P. Information from the NCS system is used as reference to define $\bar{\xi}_\alpha(H|V/C)$.

PRINCIPAL HUE CURVES OF NCS SYSTEM

Standard color chips of the NCS Atlas[8] are denoted by three parameters (s, c, ϕ), where $s(0 \sim 100)$ represents blackness, $c(0 \sim 100)$ chromaticness, and ϕ position on the NCS hue circle. The hue circle consists of quadrants of equal size, Y–R, R–B, B–G, and G–R, clockwise from the direction of 12. In each quadrant, ϕ varies from 0–100. Hence, specification (1040–R20B) means that $s = 10$, $c = 40$, and $\phi = 20$ from R to towards B, i.e., a whitish purple, not very saturated. To my best knowledge, the most detailed description of NCS color spacing is given in Tonnquist,[9] Steen,[10] Hård, Sivik, and Tonnquist,[11,12] and an experimental check is reported in Neely.[13]

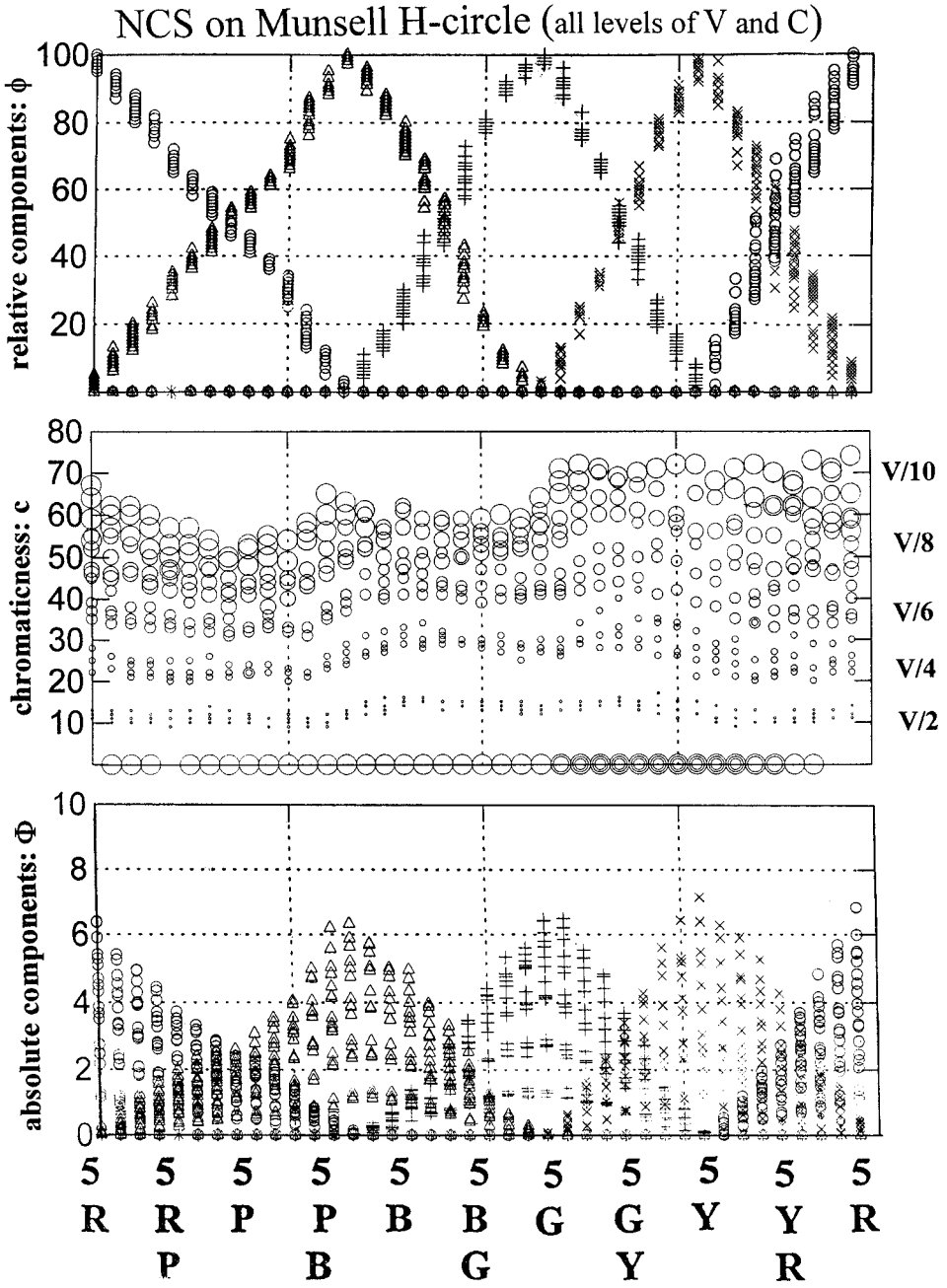

FIG. 2. Natural Color System codes on Munsell Hue-circle.

Through Table NCD ↔ Munsell,[14] (H, V/C) were converted to "exact" (s, c, ϕ) for matte finish samples, e.g., (5R 6/10) to (1870−Y39R). Let us denote the last two variables as $\phi_R = 61$ and $\phi_Y = 39$. When a unique hue α is "pure," $\phi_\alpha = 100$, for all levels of s and c. Hence, 0.01 NCS $\phi_\alpha(0 \sim 1)$ corresponds to the relative principal hue component $\eta_\alpha(0 \sim 1)$. In order to have an NCS variable that corresponds to the absolute principal hue component $\xi_\alpha(0 \sim 10)$, ϕ_α was converted to $\Phi_\alpha = (c\phi_\alpha)/1000$. Then, Φ_α varies from 0 to a maximum that depends upon s and c. Figure 2 shows ϕ_α(H|V/C), c(H V/C), and Φ_α(H|V/C) plotted against H for colors including all levels of V and C. Compared with η_α(H|V/C) of 4 hue case (Fig. 5 in II[2]), ϕ_α(H|V/C) are more independent of V and C. Both Φ_α(H|V/C) and ϕ_α(H|V/C) are more symmetric and steeper around the respective peaks than ξ_α(H V/C) and η_α(H V/C) are.

PRINCIPAL HUE CURVES $\bar{\xi}_\alpha$(H|V/C) OF SURFACE COLOR

The original idea was to define most reliable curves $\bar{\xi}_\alpha$(H|V/C) in each level of V/C by plotting ξ_α(H V/C) and Φ_α(H V/C) together on the H-circle of V/C. If ξ_α(H V/C) and Φ_α(H V/C) are proportional, then these form single curves on the respective H-circles, provided that the two units are appropriately adjusted. However, the relationship between ξ_α(H V/C) and Φ_α(H V/C) turns out to be not that simple. As an example, ξ_α(H|4/4) and φ_α(H|4/4) are plotted separately in Fig. 3(A).

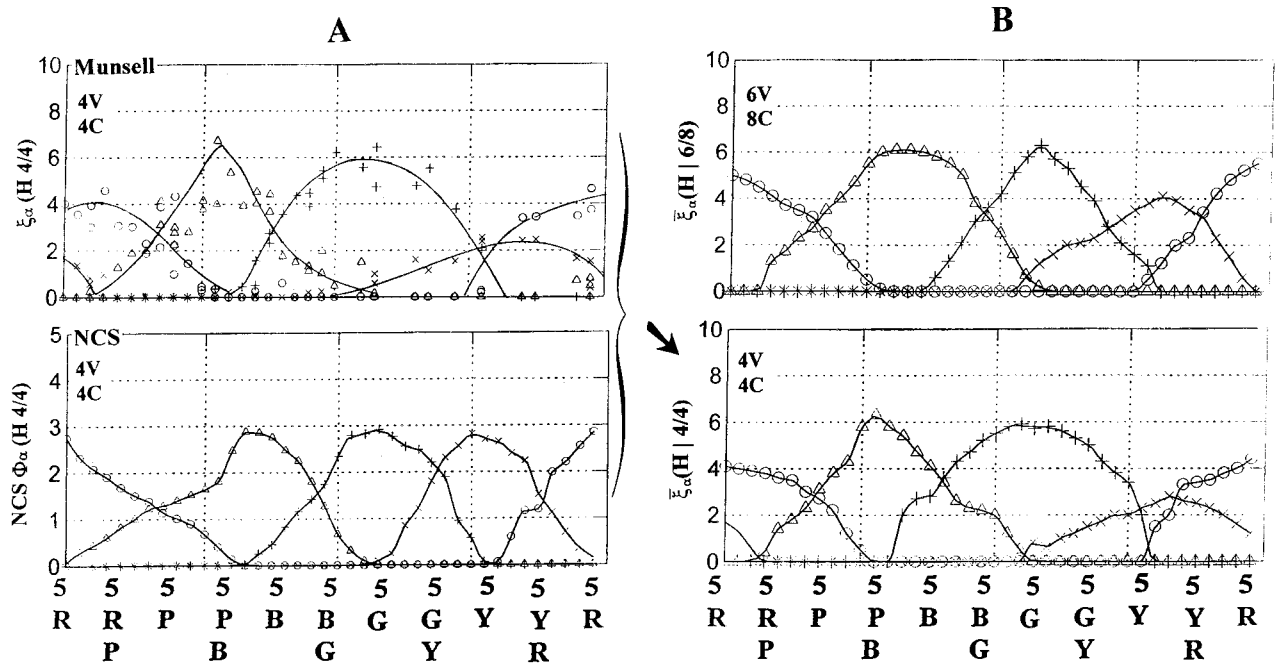

FIG. 3. Examples of absolute principal hue components on Munsell Hue-circle.

Each curve is simple smoothing of plotted points. Figure 4 shows two plots $\zeta(j)$ vs. NCS $s(j)$ and $\xi_R(j)$ vs. NCS $\Phi_R(j)$, for all (H_j V_j/C_j). Different symbols are used according to C_j. The curvilinear relationships reveal the difference in the color-spacing principle of the two systems. In this context, it will suffice to state that, in order to smooth data $\xi_\alpha(H|V/C)$, whenever necessary, plots $\Phi_\alpha(H|V/C)$ were referred to. Most reliable curves $\bar{\xi}_\alpha(H|V/C)$ were thus defined. The lower plot in Fig. 3(B) shows $\bar{\xi}_\alpha(H|4/4)$ that are based on the two plots in A on the left. In order to show how $\bar{\xi}_\alpha(H|V/C)$ change according to V/C, $\bar{\xi}_\alpha(H|6/8)$ are given above. Except for $\bar{\xi}_Y$, peak values of $\bar{\xi}_\alpha$ do not change much between 4/4 and 6/8. However, $\bar{\xi}_G$ covers a larger area of H in 4/4, whereas $\bar{\xi}_B$ is wider in 6/8. On the other hand, $\bar{\xi}_R$ remains almost the same. Around 5Y and 5GY, $\bar{\xi}_Y(6/8)$ is considerably larger than $\bar{\xi}_Y(4/4)$.

Since change of $\bar{\xi}_\alpha(H|V/C)$ according to V/C is complicated, all $\bar{\xi}_\alpha(H|V/C)$, from 4–7V and from 2–10C, are separately given in Fig. 5. Plotted points are simply connected. Irregularities in curves $\bar{\xi}_\alpha(H|V/C)$ may stem, in addition to errors in original data $\xi_\alpha(j)$ from two sources, from inappropriate color spacing with a Munsell H-sheet (V, C), if any. If a color is too saturated for its C value, it causes irregularity in the vertical direction, whereas an inappropriate Munsell H spacing affects the position of $\bar{\xi}_\alpha(H|V/C)$ on the H-continuum. As in an example of Fig. 3(A), $\bar{\xi}_\alpha(H|V/C)$ are based on plotted data points $\xi_\alpha(H\ V/C)$. The curves $\bar{\xi}_\alpha(H|4/2)$ at the top left of Fig. 5 were defined in this way. Data $\xi_\alpha(H|V/2)$ at other levels of V were too sparse to formulate $\bar{\xi}_\alpha(H|V/2)$ separately. Because NCS $\Phi_\alpha(H|V/2)$ curves are almost invariant across V, the curves $\bar{\xi}_\alpha(H|4/2)$ were assumed to hold for other V levels as $\bar{\xi}_\alpha(H|V/2)$. At higher levels of C, there are many cases in which $\bar{\xi}_\alpha(H) = 0$. In most cases, this is because chips are not available. In some cases, it is due to the lack of data.

Curves of relative principal hue components on H-circle at V/C, $\bar{\eta}_\alpha(H|V/C)$, are defined as follows:

$$\bar{\eta}_\alpha(H|V/C) = \bar{\xi}_\alpha(H|V/C)/\bar{\zeta}_\alpha(H|V/C),$$
$$0 \le \bar{\eta}_\alpha(H|V/C) \le 1, \qquad (1)$$
$$\bar{\zeta}(H|V/C) = \sum_\alpha \bar{\xi}_\alpha(H|V/C).$$

The plot of $\bar{\zeta}(H|V/C)$ on H-circle including all levels of V/C exhibits more irregular patterns than NCS $c(H|V/C)$ in Fig. 2.

Reference 2 discussed the kinds of information on the appearance of a color (H V/C) that could be obtained from curves $\hat{\xi}_\alpha(H|V/C)$ and $\hat{\eta}_\alpha(H|V/C)$. Curves $\bar{\xi}_\alpha(H|V/C)$ and $\bar{\eta}_\alpha(H|V/C)$ can be used in the same way. In the subsequent sections, another use of the curves is discussed.

PREDICTIONS OF PERCEPTUAL COLOR DIFFERENCES

Before, prediction of the color difference between (j, k), $\tilde{d}_{jk}$, and prediction of absolute principal components, $\tilde{\xi}(j)$, in a color j were, respectively, made from $\hat{d}_{jk}$ and $\hat{\xi}_\alpha(j)$ in Fig. 1(C). These predictions are directly affected by inadequacies, if any, in the current Munsell color spacing (H V/C). The size of difference the observer sees between (H_j V_j/C_j) and (H_k V_k/C_k) must be related to the differences in the respective perceived principal hues and the difference of V between j and k. Namely,

$$\tilde{d}_{jk} = \mathrm{F}(\Delta\theta_\alpha\text{'s}, \Delta\mathrm{V})$$

$$\Delta\theta_\alpha = |\theta_\alpha(\mathrm{H}_j|\mathrm{V}_j/\mathrm{C}_j) - \theta_\alpha(\mathrm{H}_k|\mathrm{V}_k/\mathrm{C}_k)|, \quad \alpha = \mathrm{R, Y, G, B},$$

$$\Delta\mathrm{V} = |\mathrm{V}_j - \mathrm{V}_k|, \tag{2}$$

where θ_α stands for either $\bar{\xi}_\alpha$ or $\bar{\eta}_\alpha$ in (1). As before, the precision of prediction is given by

$$\mathrm{RMS} = \left\{\frac{1}{N}\sum_{j,k}(d_{jk} - \tilde{d}_{jk})^2\right\}^{0.5}, \tag{3}$$

where N is the number of pairs (j, k). This prediction is only indirectly affected by possible inadequacies in the current Munsell spacing (H V/C). The reason RMS rather than the correlation r between d and $\tilde{d}$ is used is that the value of r critically depends upon the ranges of variables, and RMS is given with the unit of data d, which is common throughout in ref. 1 and the present article.

Linear Regression

Because $\Delta\mathrm{V}$ and $\Delta\theta_\alpha$ defined in the standard plane $(\mathrm{H}, \mathrm{C})_0$ are orthogonal components, let us begin with predictions of 2-D difference d_{jk}(H,C) in which $\mathrm{V}_j = \mathrm{V}_k = \mathrm{V}$ and $\Delta\mathrm{V} = 0$. According to pair (j, k), V varies in the range of 4–7. In Table II of the preceding study,[1] predictions $\tilde{d}_{jk}$(H,C) were defined and compared with data d_{jk}(H,C) separately in five regions in (H,C), **R**(5RP ~ 5YR), **Y**(5YR ~ 5GY), **G**(5GY ~ 5BG), **B**(5BG ~ 5PB), and **P**(5PB ~ 5RP). For example, all colors j in **R** are more or less reddish, but can be either bluish or yellowish as well. In addition to these five datasets, four datasets (d_{jk}(H,C)) will be considered: **RY**(5R ~ 5Y), **YG**(5Y ~ 5G), **GB**(5G ~ 5PB), and **BR**(2.5PB ~ 5R). Only two principal hues are predominant for colors in these regions. For example, for (j, k) both being in **RY,** d_{jk}(H,C) are decomposed into $\Delta\xi_\mathrm{R}$ and $\Delta\xi_\mathrm{Y}$, and all other $\xi_\alpha(j) = \xi_\alpha(k) = 0$. Figure 6 shows plots of data d_{jk}(H,C) in **RY** and in **GB** against the two relevant $\Delta\xi_\alpha$. The surfaces in A are the results by the distance weighted least squares smoothing that gives best fits to all local groups of data points, whereas those in B and C are the results of quadratic and linear smoothing for all the data points. These plots for all data sets (d_{jk},(H,C)) make two facts clear. First, it is difficult to point out any clear effect upon d_{jk}(H,C) of the interaction between $\Delta\theta_\alpha$. Second, when all relevant $\Delta\theta_\alpha$ are close to zero, d_{jk}(H,C) tend to remain at a level far above zero. Hence, let us start from linear regressions with positive intercepts:

L.R on $\Delta\bar{\xi}_\alpha$

$$\tilde{d}(\mathrm{H,C}) = d_0 + \Gamma(\Delta\bar{\xi}_\alpha),\ \Gamma(\Delta\bar{\xi}_\alpha) = \sum_\alpha a_\alpha\Delta\bar{\xi}_\alpha \tag{4}$$

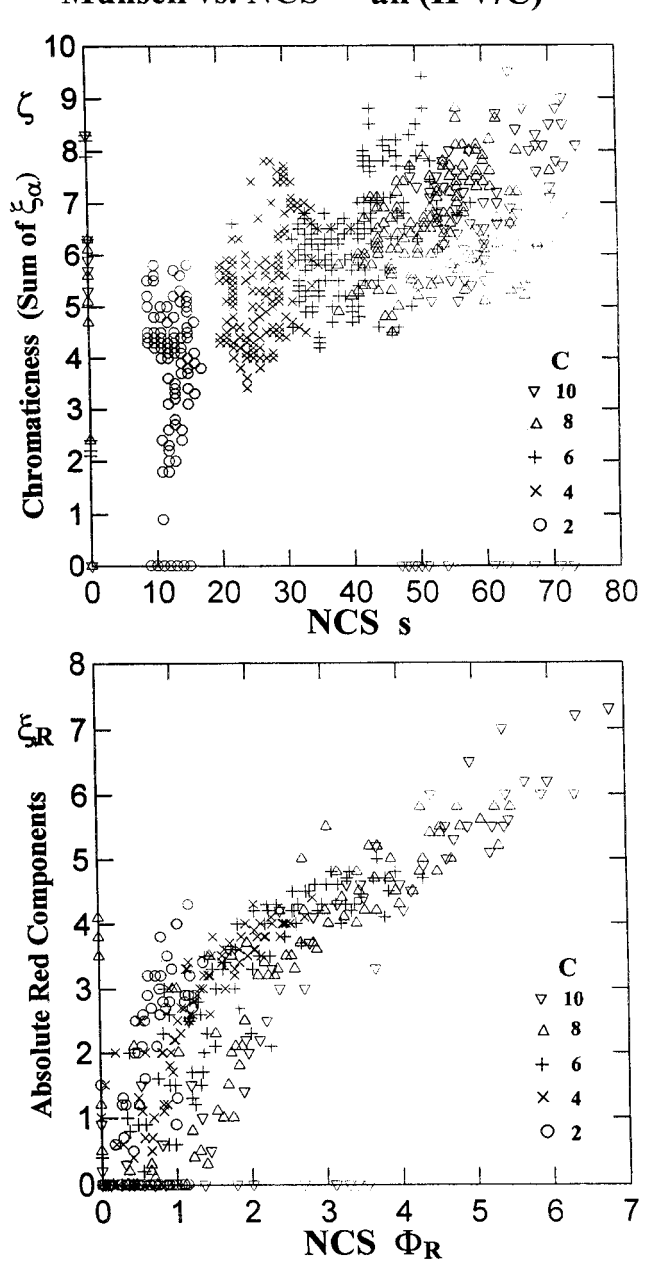

FIG. 4. Two examples of relationship between Munsell and Natural Color System codes.

L.R on $\Delta\bar{\eta}_\alpha$ $\quad \tilde{d}(\mathrm{H,C}) = d_0 + \Gamma(\Delta\bar{\eta}_\alpha)$,

$$\Gamma(\Delta\bar{\eta}_\alpha) = a_\zeta\Delta\zeta + \sum_\alpha a_\alpha\Delta\bar{\eta}_\alpha. \tag{5}$$

The term $\Gamma(\Delta\theta_\alpha)$ represents the effect of $\Delta\theta_\alpha$'s upon d, and d_0 is the pedestal constant. The plane in Fig. 6(C) represents (4).

Table I gives the results of fittings for 2-D color differences datasets (d_{jk}(H,C)), those of (4) in columns from 4–9, and those of (5) in the columns that follow. There were some cases (j, k) in which C or V of either color was out of the range of Fig. 5, e.g., 5Y 7/12, 7.5Y 8/10, or 2.5RP 4/12. It occurs for

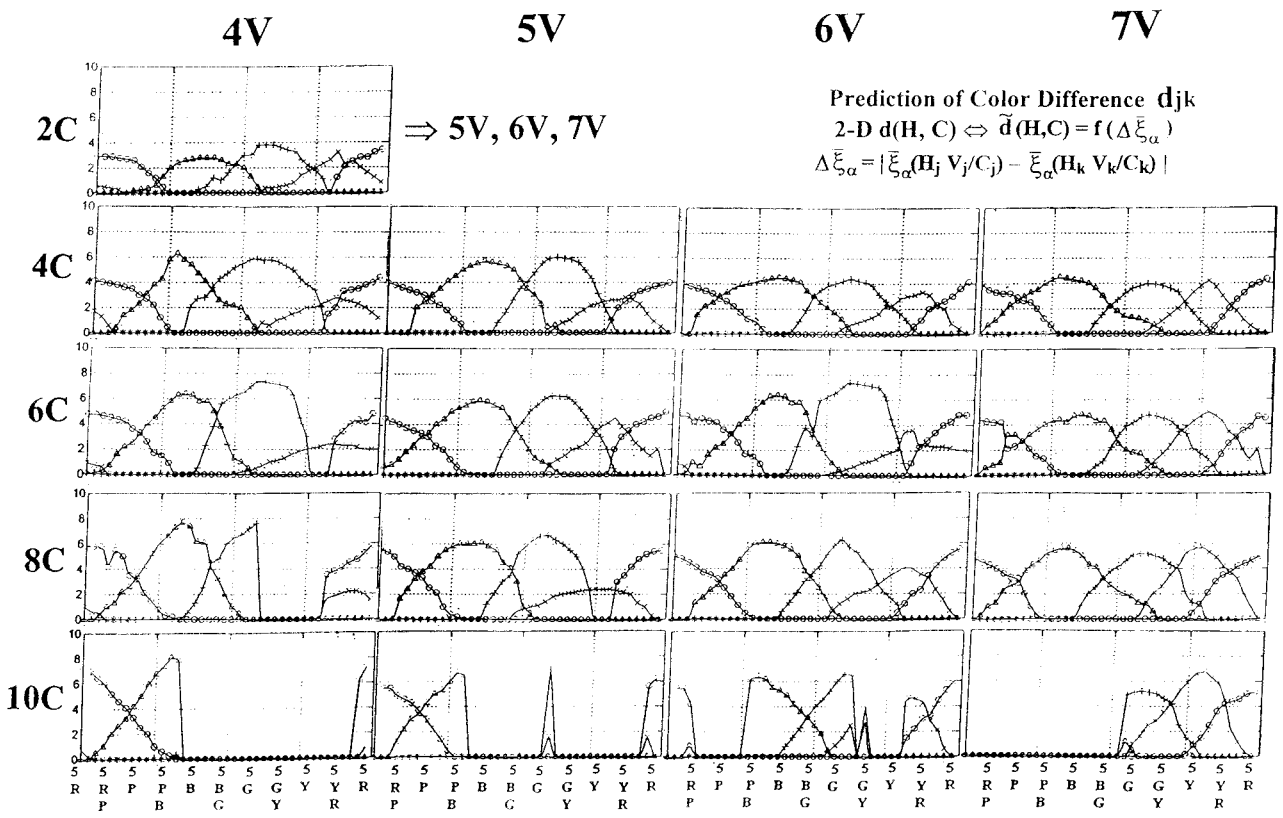

FIG. 5. Standardized principal hue curves on Munsell Hue-circle.

colors in Y- or B- region, and $\bar{\xi}_\alpha$ of these colors were estimated by extrapolating $\bar{\xi}_\alpha$(H|V/C) in Fig. 5. In each region, only relevant principal hue terms α are taken into account, three for **R**, **Y**, **G**, **B**, **P**, and two for **RY**, **YG**, **GB**, **BR**. The dataset **ALL** means the all pairs (j, k) in which $V_j = V_k$, and α = R, Y, G, and B in this case. For the sake of comparison, RMS, the scatter of data points around $\tilde{d}(\hat{d})$, are included in column 3 (Table II in ref. 1), where the predictor $\hat{d}$ is distance in the current Munsell solid.

1. Except in the regions **R**, **Y**, RMS of $\tilde{d}(\Delta\bar{\xi}_\alpha)$ in column 4 are significantly smaller than RMS of $\tilde{d}(\hat{d})$ in column 3. Though test of significance is not too important in this context, it can be performed in the following way. Consider two independent S_A and S_B, sums of squares with degree of freedoms, f_A and f_B, then

$$F = \frac{S_A}{f_A} \Big/ \frac{S_B}{f_B} > 1$$

   is distributed according to the F-distribution of degrees of freedom, f_A and f_B. Herein, if scatters of N points are regarded as random variables normally distributed around zero,
   $S = N \times \mathrm{RMS}^2$,

   $f = N -$ (the number of parameters estimated).

   Then, F = 1.20 for **ALL**, 2.03 for **G**, and 1.67 for **B**, and these are beyond the levels of significance of 0.05 or 0.01 under the respective degrees of freedom. In **R** and **Y**, RMS in the forth column is slightly larger, but none of the differences is significant (F = 1.23 for **R** and 1.05 for **Y**). Hence, we can conclude that $\tilde{d}(\Delta\bar{\xi})$ of (4) gives about the same or slightly better results than $\tilde{d}(\hat{d})$ in the previous article.[1]
2. Fits of $\tilde{d}(\Delta\bar{\eta})$ are consistently poorer in spite of the fact that Eq. (5) has one additional free parameter. The fitting was tried with four hues in regions **R**, **Y**, **G**, **B**, and **P** (the second block of rows). No systematic reduction of RMS was observed. Furthermore, a_α turned out to be negative in some cases. Hence, we can conclude that assessment of color difference d_{jk} is not based on ($\Delta\zeta$, $\Delta\bar{\eta}_\alpha$), and hereafter Eq. (5) will not be discussed.
3. The data "3-D All Hues" (row 7 of Table II[1]), where $V_j \neq V_k$ in all pairs, were analyzed in the same way with an additional term $a_\alpha\Delta V$ on the right side of Eq. (4). The result is given at the bottom. The size of RMS (= 0.536) is much smaller than RMS (= 0.625) for $\tilde{d}(\hat{d})$ in the previous study, and also smaller than RMS (= 0.582) when the predictor is CIE94. Among the four color difference formulae, CIE94 gave the best result (Table II in ref. 1).
4. The contribution to $\tilde{d}(\Delta\bar{\xi})$ of red difference, a_R, tends to be large, whereas those of yellow and blue differences, a_Y and a_B, tend to be small.

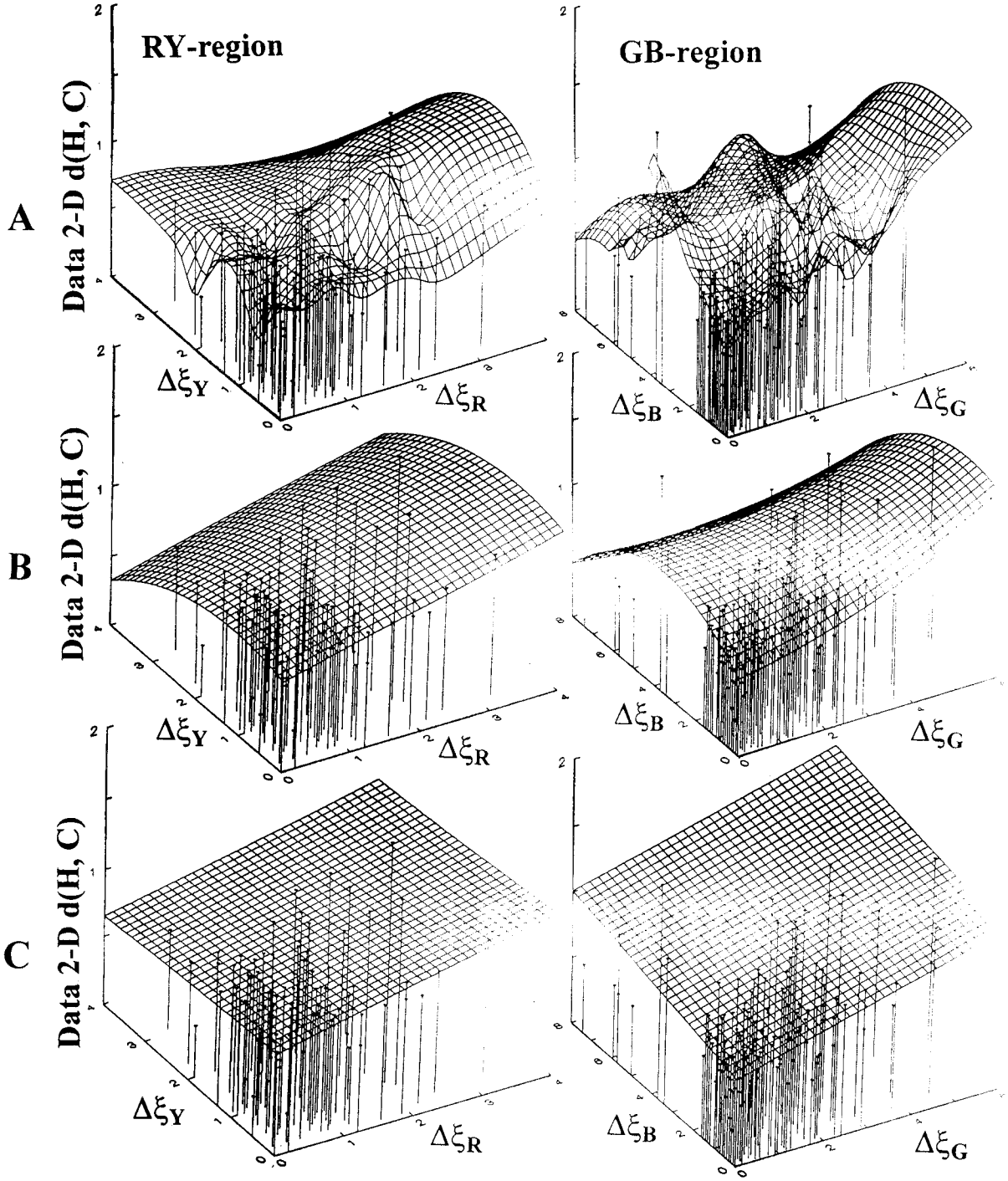

FIG. 6. Two examples of 2-D color differences plotted against two differences of related principal hues. (A) Distance weighted least squares smoothing; (B) Quadratic smoothing; (C) Linear smoothing.

5. In contrast to that $\tilde{d}(\hat{d})$ is proportional to $\hat{d}$ (Figs. 2, 3, in I), we must include a positive intercept d_0 in $\tilde{d}(\Delta\bar{\xi})$. Figure 7(A) shows the plots of d_{jk} against $\Gamma_{jk}(\Delta\bar{\xi}_\alpha)$ of the dataset **ALL** of 2-D color differences. The straight line represents the regression line $\tilde{d}(\Delta\bar{\xi})$ of (4) with $d_0 = 0.620$. Deviations of points from this line are shown in Fig. 7(B). As in this plot, if deviations are almost constant in all levels of the predictor, the fit is called *unbiased.* The standard deviation of these deviations is what is called RMS (0.282) in Table I. The broken straight line and the curve in A, both passing through the origin, are explained below.

Nonlinear Forms

In Fig. 7(A), the broken straight line represents the proportionality (slope = 2.69), and its fit is unacceptable for two reasons. Deviations of points from this line are very biased and RMS (0.447) is much larger. Even if parameters a_α are estimated under the constraint of d_0 being zero in (4),

TABLE I. Linear regression, (4) and (5).

			2-D differences ($V_j = V_k$)												
$\tilde{d}(\hat{d})$			$\tilde{d}(\Delta\bar{\xi}_\alpha)$, (4)						$\tilde{d}(\Delta\bar{\eta}_\alpha)$, (5)						
1	2	3	4	5	6	7	8	9	10	11	12	13	14	15	16
	N	RMS	RMS	d_0	a_R	a_Y	a_G	a_B	RMS	d_0	a_ζ	a_R	a_Y	a_G	a_B
R	164	0.239	0.263	0.653	0.186	0.045		0.097	0.281	0.749	0.081	0.011	0.111		0.538
Y	145	0.269	0.273	0.689	0.075	0.059	0.113		0.274	0.713	0.022	0.227	0.470	0.467	
G	109	0.302	0.209	0.637		0.121	0.095	0.057	0.214	0.702	0.008		0.334	1.000	−0.177
B	175	0.362	0.278	0.615	0.442		0.110	0.033	0.294	0.653	0.021	2.040		0.359	0.304
P	124	0.307	0.257	0.543	0.223	0.108		0.085	0.270	0.644	0.023	1.279	0.669		0.034
ALL	717	0.299	0.282	0.620	0.223	0.047	0.105	0.070	0.298	0.729	0.021	0.117	0.259	0.265	0.660
R	164	0.239	0.263						0.261	0.732	0.088	−0.112	0.121	1.33	0.653
Y	145	0.269	0.273						0.273	0.720	0.023	0.191	0.406	0.543	−0.318
G	109	0.302	0.208						0.210	0.697	0.015	1.421	0.581	0.600	0.096
B	175	0.362	0.278						0.293	0.657	0.019	1.940	−1.508	0.485	0.406
P	124	0.307	0.257						0.270	0.644	0.023	1.279	0.669	0	0.034
RY	156		0.200	0.641	0.114	0.053									
YG	104		0.270	0.688		0.110	0.088								
GB	223		0.224	0.639			0.094	0.046							
BR	254		0.297	0.545	0.336			0.063							

			3-D differences ($V_j \neq V_k$)						
$\tilde{d}(\hat{d})$			$\tilde{d}(\Delta\bar{\xi}_\alpha, \Delta V)$, (4)						
	N	RMS	RMS	d_0	a_V	a_R	a_Y	a_G	a_B
ALL	241	0.625	0.536	0.732	0.408	0.176	0.023	0.086	0.228

the situation is essentially the same. A simple way to eliminate d_0 in (4) is to intervene a nonlinear relationship between d and $\Gamma(\Delta\bar{\xi}_\alpha)$. The curve in Fig. 7(A) shows an example of such an attempt in which

Power Function $\tilde{d}(\mathrm{H, C}) = \mathrm{A}\{\Gamma(\Delta\bar{\xi}_\alpha)\}^{\mathrm{B}}$,

$$\Gamma(\Delta\bar{\xi}_\alpha) = \sum_\alpha a_\alpha \Delta\bar{\xi}_\alpha \quad (6)$$

is used. Using two free parameters, A and B, in (6) gives the same level of RMS as using one parameter d_0 in (4). However, deviations of points from this curve (6) were very biased. Even when all a_α were optimized according to the form of (6), the result was essentially the same. Other intervening forms, such as logarithmic or negative exponential functions and Minkowski's metric, were tried. No improvement of fits over Table I was obtained.

Instead of linear combination $\Gamma(\Delta\xi_\alpha)$, various forms of nonlinear combination of $a_\alpha\Delta\bar{\xi}_\alpha$ were tested. The results of only two forms are given in Tables II and III with 2-D difference datasets in Table I.

L.R. on Logarithmic Terms

$$\tilde{d}(\mathrm{H, C}) = d_0 + \sum_\alpha a_\alpha \log \Delta\bar{\xi}_\alpha \quad (7)$$

L.R. on Powered Terms

$$\tilde{d}(\mathrm{H, C}) = d_0 + \sum_\alpha a_\alpha \Delta\bar{\xi}_\alpha^{b_\alpha}. \quad (8)$$

Equation (7) is a standard form, if $\Delta\xi_\alpha$ are regarded as ratio scales and $\tilde{d}_{jk}(\mathrm{H, C})$ as an interval scale.[15,16] Table II shows fits of (7) and, for the sake of comparison, the values of RMS for (4) in Table I are included in the column under $\tilde{d}(\Delta\xi_\alpha)$. Though deviations are unbiased, RMS's for (7) (column 4) are consistently larger than those for $\tilde{d}(\Delta\bar{\xi}_\alpha)$ of (4), even when the slope coefficient is included in front of

TABLE II. 2-D color difference, linear regression on logarithmic terms (7) (with slope).

$\tilde{d}(\Delta\bar{\xi}_\alpha)$			$\tilde{d}(a_\alpha \log \Delta\bar{\xi}_\alpha)$, $d_0 > 0$						
	N	RMS	RMS	Slope	d_0	a_R	a_Y	a_G	a_B
R	164	0.263	0.322	1.000	1.016	0.151	0.130		0.024
Y	145	0.273	0.302	0.950	0.986	0.095	0.122	0.131	
G	109	0.208	0.234	0.844	1.067		0.021	0.058	0.203
B	175	0.278	0.358	0.951	1.019	0.221		0.060	0.185
P	124	0.257	0.288	1.033	0.902	0.119	0.178		0.106
ALL	717	0.282	0.305	0.739	1.251	0.210	0.025	0.136	0.108
RY	156	0.200	0.243	0.580	1.459	0.138	0.237		
YG	104	0.270	0.278	0.959	0.981		0.086	0.114	
GB	223	0.224	0.258	0.792	1.008			0.108	0.072
BR	254	0.297	0.359	1.082	0.928	0.210			0.109

TABLE III. 2-D color difference, linear regression on powered terms (8).

	$\tilde{d}(\Delta\bar{\xi}_\alpha)$		$\tilde{d}(a_\alpha\Delta\bar{\xi}_\alpha^{b_\alpha})$, $d_0 = 0$									$d_0 > 0$
	N	RMS	RMS	a_R	b_R	a_Y	b_Y	a_G	b_G	a_B	b_B	RMS
R	164	0.263	0.385	0.477	0.886	0.380	0.935			0.447	0.696	0.261
Y	145	0.273	0.445	0.370	1.003	0.303	0.946	0.286	0.702			0.272
G	109	0.208	0.370			0.253	0.895	0.311	0.686	0.329	0.937	0.208
B	175	0.278	0.415	0.341	1.080			0.272	0.901	0.322	0.363	0.271
P	124	0.257	0.391	0.311	1.000	0.298	0.993			0.303	0.557	0.255
ALL	717	0.282	0.381	0.540	0.801	0.299	1.104	0.537	0.201	0.199	0.805	0.270
RY	156	0.200	0.378	0.647	0.839	0.205	0.954					0.265
YG	104	0.270	0.479			0.280	0.576	0.350	0.981			0.271
GB	223	0.224	0.445					0.341	0.876	0.163	1.156	0.223
BR	254	0.297	0.367	0.292	1.401					0.636	0.111	0.294

the second term Σ on the right side of (7). Table III summarizes fits of Eq. (8). Again, RMS's for (4) in Table I are included in the column under $\tilde{d}(\Delta\bar{\xi}_\alpha)$. Columns 4–12 give results when d_0 is fixed at 0 in (8). Though fits are not biased, RMS's for (8) with $d_0 = 0$ are consistently larger than those in column 3, in spite of the fact that a large number of free parameters are involved. In the last column RMS's for (8) with d_0 (>0) are given. These RMS's are of the same level with or only slightly smaller than those for $\tilde{d}(\Delta\bar{\xi}_\alpha)$ of (4) (column 3).

In Eq. (2), it is possible to think of ratios $\theta_\alpha(H_j|V_j/C_j)/\theta_\alpha(H_k|V_k/C_k)$ or some other forms in place of differences $\Delta\theta_\alpha$. Ratios are not definable or unstable when one θ_α is either zero or close to zero. For some purely reddish colors j in region **RY**, $\theta_Y(j) = 0$. In general, ratios are found not stable. Hence, it is concluded that the best predictor of 2-D color difference is $\tilde{d}$(H, C) of (4), which is based on differences $\Delta\xi_\alpha$.

STANDARD DATASET OF 2-D AND 3-D COLOR DIFFERENCES

The results of linear regression of the set of 3-D differences ($V_j \neq V_k$) was given at the bottom of Table I. For all pairs in this set $\Delta V > 0$. In practice, we have to deal with dataset (d_{jk}) in which either $V_j = V_k$ or $V_j \neq V_k$. Hence, a standard dataset was assembled from all the data in Table I of ref. 1 under the following constraint. It was noticed[1] that the proportionality between d_{jk} and $\hat{d}_{jk}$ is different when (j, k) are such pairs in which one is gray and the other is a color of 2C. In any hue direction, the first step $\Delta C = 2$ from the gray tends to appear about 1.3 times larger than two chromatic colors having $\hat{d}_{jk} = 2$. Beside, as stated before $\bar{\xi}_\alpha(H|V/C)$ for other V levels than 4V in Fig. 5 are not based on real data. Hence, all cases in which $\bar{\xi}_\alpha(H|V/C)$ is paired with a gray of V were excluded. Furthermore, when two colors are too far apart in the Munsell solid, the observer cannot convert the perceptual difference δ to matched V difference d with confidence. Hence, all pairs in which $\Delta V \geq 3$ or $\Delta C \geq 6$ were excluded. Then, the remaining data (d_{jk}) are called the standard dataset ($N = 899$) which consist of 2-D differences ($V_j = V_k$), $N = 706$, and 3-D differences ($V_j \neq V_k$), $N = 193$.

Figure 8(A) is the scatter diagram of the same kind as Figs. 1 and 3 in ref. 1. The abscissa $\hat{\hat{d}}$ is defined from ΔV, the difference of V, and $\hat{d}$(H,C), distance in the Munsell plane of constant V (Fig. 1), with r(V/C) and K(□)'s given in the legend.

$$\hat{\hat{d}} = 0.357\{(r(V/C)\Delta V)^2 + [K(\square)\hat{d}(H,C)]^2\}^{0.5}. \quad (4) \text{ in I}$$

Then, d is predicted by $\tilde{d} = (0.971)\,\hat{\hat{d}}$, and the RMS of the scatter of points around this line is 0.364. Figure 8(B) shows the proportionality between data d and

$$\tilde{d}(\Delta V, \Delta\bar{\xi}) = d_0 + a_V\Delta V + \Gamma(\Delta\bar{\xi}),$$

$$\Gamma(\Delta\bar{\xi}) = \sum_\alpha a_\alpha\Delta\bar{\xi}_\alpha. \quad (9)$$

$$d_0 = 0.610,\ a_V = 0.459,\ a_R = 0.199,$$

$$a_Y = 0.031,\ a_G = 0.098,\ a_B = 0.136.$$

These parameter values are optimized with regard to this set of data. If values of a_V and a_α are optimized without including d_0, the RMS increases to 0.538 and deviations are highly biased. In contrast to Fig. 7 in which the abscissa is $\Gamma(\Delta\bar{\xi})$, the abscissa of Fig. 8(B) is $\tilde{d}$ with $d_0 = 0.610$, hence d is proportional to $\tilde{d}$ with the slope of 0.999, with RMS = 0.338. As predictor of d, $\tilde{d}$ of (9) [Fig. 8(B)] gives RMS slightly smaller than $\hat{\hat{d}}$ [Fig. 8(A)]. As the curve of Eq. (6) in Fig. 7, if d_{jk} is fitted by a power function of $(a_V\Delta V_{jk} + \Gamma_{jk}(\Delta\bar{\xi}_\alpha))$,

$$\tilde{d} = A(a_V\Delta V + \Gamma(\Delta\bar{\xi}_\alpha))^B,$$

$$A = 1.597, \quad B = 0.408, \quad (10)$$

when RMS = 0.361 and deviations are unbiased, Even if (10) is fitted by optimizing al the parameter values, A, B, a_V, and a_α, the results is essentially the same (RMS = 0.357). Using two free parameters (A, B) instead of one (d_0) does not reduce RMS beyond that for Eq. (9).

Figure 8(C, D) shows the results for pairs that are not included in the standard dataset, because one is gray and the other is of 2 C ($N = 31$). The abscissas are the same with A and B, respectively. The broken lines represent the proportionality relationship in A and B, and the unbroken lines

show the proportionality fitted to these scatter diagrams C and D. As expected, there are systematic differences in proportionality between A and C as well as B and D.

It is interesting to test with this standard dataset the following nonlinear combination of effects:

Minkowski type combination

$$\tilde{d} = \{(a_V \Delta V)^r + \tilde{d}(\mathrm{H, C})^r\}^{1/r}. \quad (11)$$

According to value of r (> 0), (11) represents for different situations. If $r = 1$, (11) is the same as (9). If $r = 2$, $\tilde{d}$ represents Euclidan distance on two orthogonal difference axes, $(a_V \Delta V)$ and $\tilde{d}$(H, C). If $r =$ infinity, $\tilde{d} = \max\{(a_V \Delta V), \tilde{d}(\mathrm{H, C})\}$. In other words, the observer pays attention only to the larger difference and completely ignores the smaller difference.[17] Of course, this is an extreme situation. If $r > 2$, however, it implies that the observer tends to put more weight to the larger one, $a_V \Delta V$ or $\tilde{d}$(H, C), in assessing the total color difference d. If $r < 1$, $\tilde{d}$ of (11) violates the triangular inequality axiom for distance, and $\tilde{d}_{ik} < (\tilde{d}_{ij} + \tilde{d}_{jk})$ for three collinear points P_i, P_j, and P_k in this order. In contrast to $\hat{d}$, it is irrelevant in this context whether $\tilde{d}$ can be regarded as a distance or not, and this subadditivity is often observed in sensory scaling. Hence, it is worthy to see if parameter r takes a value clearly smaller than 1 or clearly larger than 1. Fitting (11) gives the following parameters values with RMS = 0.337:

$$r = 1.134,\ a_V = 0.550,\ \text{and in } \tilde{d}(\mathrm{H, C}),$$

$$d_0 = 0.592,\ a_R = 0.238,\ a_Y = 0.053,$$

$$a_G = 0.119,\ a_B = 0.169.$$

Even if the initial value for r is set equal to 0.5 or 5 in the optimization process, the final results always came back to the parameter values shown above. That r is close to 1 means that the situation is essentially represented by Eq. (9), and we can conclude that a simple linear equation with a pedestal constant d_0 holds between d and $\Delta\bar{\xi}_\alpha$, both based on assessment.

The necessity of d_0 (0.62) in (4) and (9) does not mean that, if pairs (j, j) of two identical colors are presented for which $\Gamma(\Delta\bar{\xi}_\alpha)$ is zero, the observer would select such pairs of gray (N_A, N_X) in which $N_A \neq N_X$ and differences $|V_A - V_X|$ are 0.62 on the average. It may happen, of course, that the observer responds with some positive values d_{jj} to the identical pairs. However, it is not likely that the RMS of these values reaches 0.6. The RMS between data d_{jk} and Euclidean distances between P_j and P_k of the configuration constructed by MDS is $0.2 \sim 0.3$ in the matched V-unit (Table II in ref. 1) and the RMS for pure matching errors cannot be larger than this level. Furthermore, the relationship between d and $\hat{\tilde{d}}$ is fairly well represented by a straight line passing through the origin [Fig. 8(A), and Figs. 1, 3 in ref. 1].

The pedestal constant stems from the difference in relationships, $\Gamma(\Delta\bar{\xi}_\alpha)$ and $\Gamma(\Delta\bar{\xi}_\alpha, \Delta V)$ vs. $\hat{\tilde{d}}$ and d vs. $\hat{\tilde{d}}$. The plot of $\Gamma(\Delta\bar{\xi}_\alpha, \Delta V)$ against $\hat{\tilde{d}}$ in Fig. 9 shows that the linear

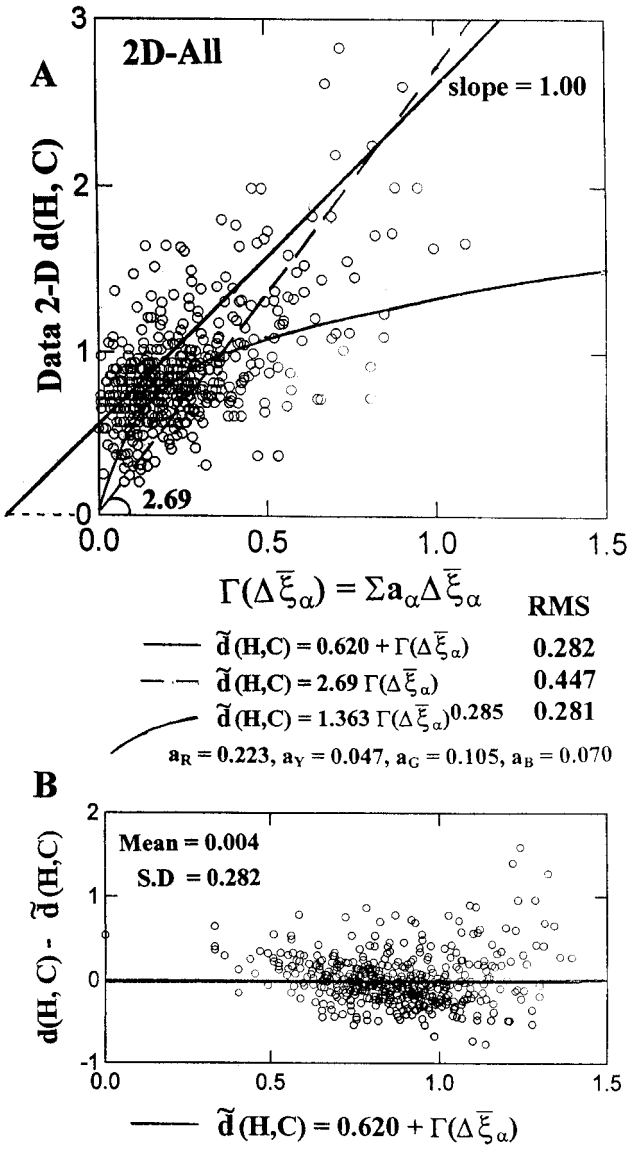

FIG. 7. 2-D color difference and linear combination of principal hue differences. (A) Scatter diagram and three representations of the trend. (B) Residuals of (4) with d_0 plotted against the predictor.

combination Γ is represented by a concave upward function of $\hat{\tilde{d}}$, whereas Fig. 8(A) shows that d is proportional with $\hat{\tilde{d}}$. Hence, data d and $\Gamma(\Delta\bar{\xi}_\alpha)$ are related, as shown in Fig. 7. If we want to represent this trend in Fig. 7 by a straight line, even if $d = 0$ and $\Gamma(\Delta\bar{\xi}_\alpha) = 0$ for $\hat{\tilde{d}} = 0$, we need a positive intercept d_0. The difference between Figs. 8(A) and 9 can be interpreted in two ways.

One interpretation is to see the following difference in responses underlying d and $\Gamma(\Delta\bar{\xi}_\alpha)$. Figure 8(A) shows that the observer can convert δ to the matched V-difference d keeping the same proportionality for the entire range of $\hat{\tilde{d}}$ under discussion. The trend in Fig. 9 can be regarded as consisting of two straight lines with different slopes. For δ in the level of $\hat{\tilde{d}} < 0.7$ or so, the observer cannot respond with such ξ_α that $\Gamma(\Delta\bar{\xi}_\alpha)$ has the same proportionality with δ as in the higher level $\hat{\tilde{d}}$. The other interpretation is to

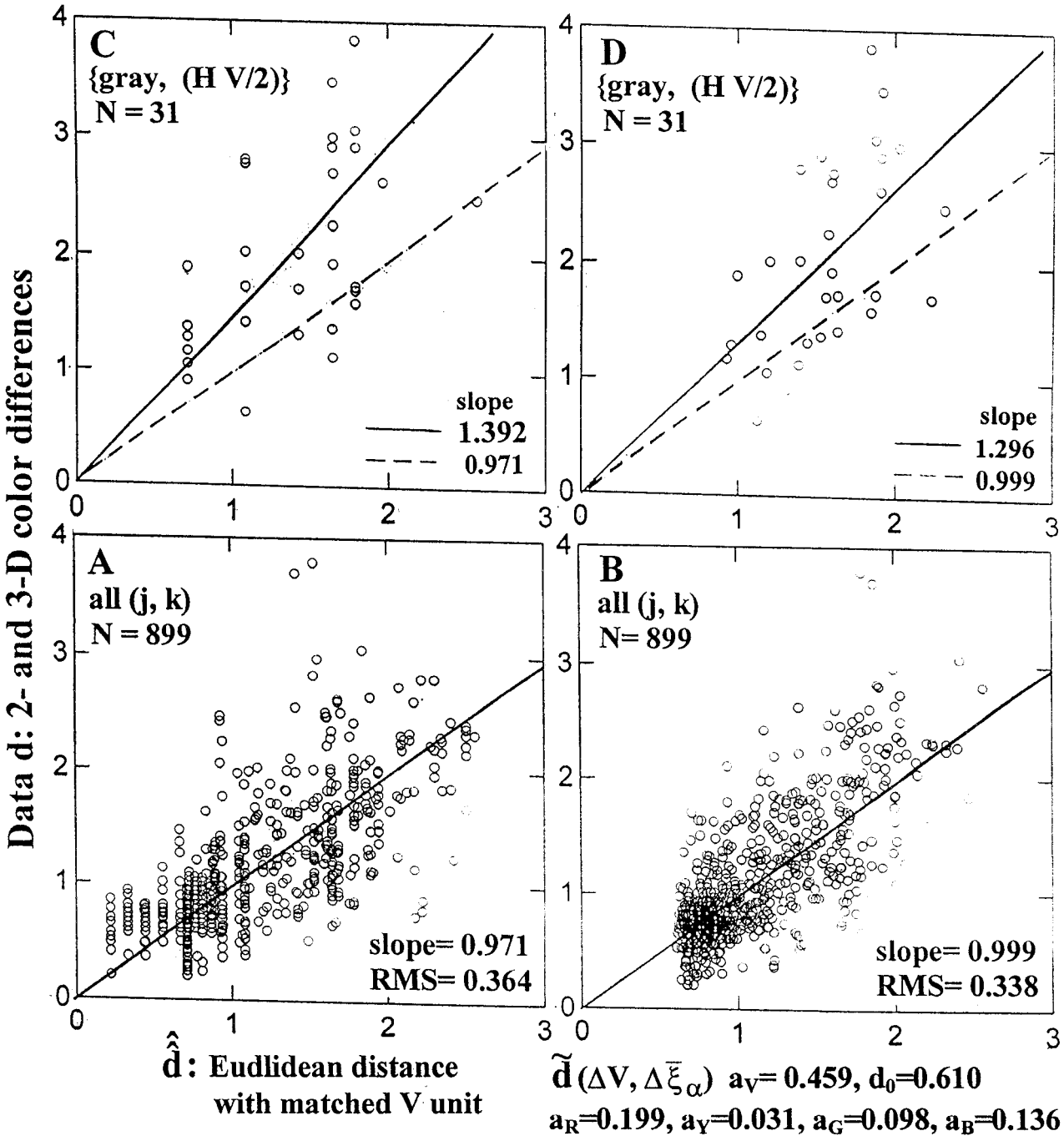

FIG. 8. 2- and 3-D color difference and two predictors. (A and B) Standard Dataset. (C and D) Pairs in which one is a gray and the other is a color of 2 C.

regard the difference as a reflection of the nonlinearity in quantitative assessment of the relationship between two quantity-like perceptions, δ's and $\mathcal{H}_\alpha$'s, etc.

In general, the quantitative assessment must be in terms of either difference or ratio relationship in quantity-like perception. In MDS studies, perceptual color difference δ was converted to data d through assessment on either difference-relationship or ratio-relationship between δ's in an experiment. Let us denote the former scale by $u(\delta)$ and the latter scale by $v(\delta)$, then the relationship with interpoint distance $\hat{d}$ in the constructed configuration was different between these two scales; $u(\delta)$ is proportional to $\hat{d}$, whereas $v(\delta)$ is an accelerated function of $\hat{d}$ (e.g., Fig. 6 in Indow and Kanazawa[18] or Fig. 3 in Indow[3]). In the present context, it is clear that data d, matched V-difference, is to be regarded as $u(\delta)$, because the Munsell V-scale has been defined by equating perceptual sizes between neighboring intervals along the gray series. Since $\hat{\hat{d}}$ is $\hat{d}$ expressed by the matched V-unit, the finding of d being proportional to $\hat{\hat{d}}$ corresponds to the proportionality between $u(\delta)$ and $\hat{d}$. On the other hand, the

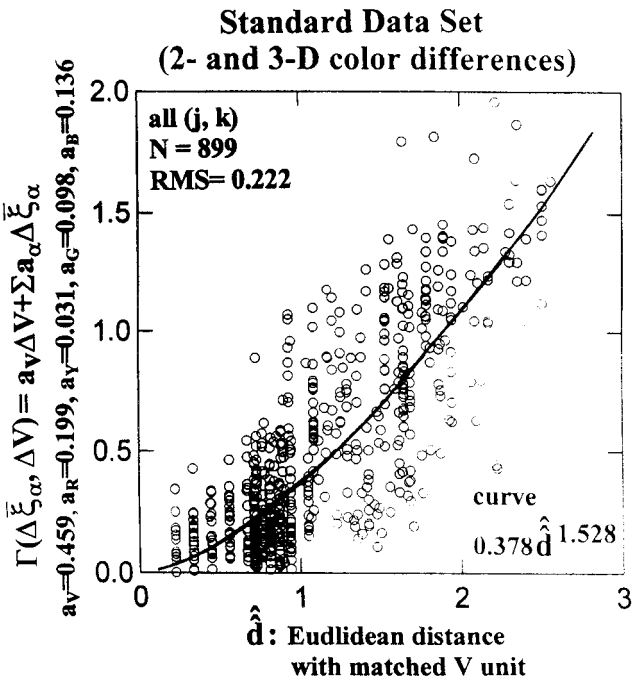

FIG. 9. Relationship between linear combination Γ of principal hue- and V-differences and Euclidean distance in Munsell solid with matched V-unit.

nature of scale $\Gamma(\Delta\bar{\xi}_\alpha)$ is not self-evident. Each term $\Delta\bar{\xi}_\alpha$ is based on data ξ_α (Fig. 1). The observer divides the segment ζ in proportion to degrees of perceptual principal hues $\mathcal{H}_\alpha$. The curvilinearity in Fig. 9 is of the same form as that between $v(\delta)$ and $\hat{d}$ in MDS studies. If $\Gamma(\Delta\bar{\xi}_\alpha)$ is interpreted as a $v(\delta)$, its curvilinearity with d as $u(\delta)$ in Fig. 7 corresponds to the functional form between u-scale and v-scale that has been widely demonstrated in many sense modalities (e.g., saturation of colors,[19] loudness of tones, brightness, sweetness in taste,[20] etc.). The NCS ϕ_α is based on ratio assessment of the degree of hue α, and hence Φ_α is to be regarded as a $v(\mathcal{H}_\alpha)$. Then, if ξ_α is regarded as a $v(\mathcal{H}_\alpha)$, the accelerated form of Φ_R against ξ_R in Fig. 4 means nonlinearity between two v-scales. In this case, the trend seems to consist of two lines with different slopes. It will be an interesting study to make explicit why two ratio assessments of the same latent variable $\mathcal{H}_R$ have yielded this curvilinearity.

Table IV shows two groups of d_{jk} of largest deviations from $\tilde{d}_{jk}$, 15 each, to the positive and negative sides in Fig. 8(B). Throughout two groups, there are many cases in which at least one color is of 2 C. It may be due to the situation that, except colors (H, 4/2), $\bar{\xi}_\alpha(\mathrm{H}|\mathrm{V/C})$ in Fig. 5 are not based on real data. Another possibility may be that assessments of low saturated colors are different from other cases. In the group ($d < \tilde{d}$), there are 7 cases in which j and k are of the same H, and the differences correspond to distances in the radial direction in the Munsell solid. In the group ($d > \tilde{d}$), pairs in **B** and **P** regions are dominant. In the group ($d < \tilde{d}$), pairs in **Y** and **GY** regions are dominant. It will be of importance to

TABLE IV. Large discrepancies between data d and prediction $\tilde{d}$, linear regression (9), (15 top and 15 bottom in 899 cases), in standard dataset.

$d - \tilde{d}$	d	$\tilde{d}$	$\hat{d}$	j	k
1.996	3.790	1.794	1.534	5PB 3/6	5P 4/4
1.824	3.696	1.871	1.417	5BG 4/2	5P 5/2
1.246	2.418	1.172	0.932	5B 3/2	5PB 4/2
1.222	2.616	1.394	1.687	5PB 3/6	5P 3/8
1.166	2.104	0.938	1.385	5GY 7/2	5BG 7/4
0.998	1.706	0.709	1.474	5GY 6/6	5G 6/7
0.974	2.973	1.999	1.558	5PB 5/6	5P 6/6
0.970	2.598	1.628	1.687	5PB 6/8	5P 6/6
0.950	2.188	1.239	2.099	7.5Y 6/10	7.5Y 6/8
0.935	2.828	1.893	1.534	5PB 5/6	5P 4/4
0.901	2.806	1.904	2.307	5BG 5/6	5B 3/2
0.892	1.643	0.751	1.358	5B 4/8	2.5PB 4/6
0.888	2.471	1.582	1.620	5PB 5/6	5P 5/2
0.880	2.052	1.172	0.932	5B 3/2	5PB 4/2
0.872	1.644	0.771	1.385	5YR 6/4	5RP 6/2
−0.725	0.942	1.667	1.534	5R 6/6	5RP 7/4
−0.726	0.649	1.376	1.088	5RP 6/2	5RP 7/4
−0.742	0.649	1.391	1.647	5YR 6/4	5YR 7/8
−0.748	0.942	1.690	1.254	5YR 5/2	5Y 6/4
−0.774	1.288	2.062	1.896	5P 5/2	5RP 7/4
−0.836	0.565	1.402	1.088	5GY 6/6	5GY 7/8
−0.837	0.387	1.224	1.088	5Y 7/6	5Y 8/8
−0.848	0.576	1.423	0.932	5Y 8/2	5GY 7/2
−0.861	0.366	1.227	0.781	7.5P 4/4	2.5RP 4/2
−0.869	0.523	1.392	1.088	5GY 7/8	5GY 8/10
−0.877	0.963	1.840	1.647	5P 5/2	5P 6/6
−0.890	0.764	1.654	1.206	5BG 7/4	5B 6/4
−0.910	1.096	2.006	1.896	5BG 4/2	5B 6/4
−0.922	0.733	1.655	2.176	5GY 6/6	5GY 8/10
−1.114	0.672	1.786	1.174	5G 4/2	5B 3/2

check the Munsell color spacing from this point of view. As to large deviations in Fig. 8(D), no special trend is found. It will be important to check the Munsell color spacing from this point of view.

In this article, the analysis has focused on the relationship between d_{jk} and a linear combination Γ of $\Delta\bar{\xi}_\alpha$'s and ΔV. It will also be interesting to carefully check the relationship between d_{jk} and $\{\bar{\xi}_\alpha(H_j|V_j/C_j))$, $\bar{\xi}_\alpha(H_k|V_k/C_k)|$ in the standard dataset from a more qualitative point of view, e.g., the set-theoretical approach by Tversky.[21]

CONCLUSION

As to colors in the main part of Munsell solid, 4–7V and 2–10C, absolute principal hue curves $\bar{\xi}_\alpha$ on H-circle (Fig. 5) give us useful information. We can tell from $\bar{\xi}_\alpha(H_j|V_j/C_j)$ how a color j appears. As such an example, the appearance of brown was discussed in II.[2] If relative principal hue components are necessary, $\bar{\eta}_\beta(H, V/C)$ can be obtained through (1) from $\bar{\xi}_\alpha(H|V/C)$. We can predict the perceptual difference for any pair of colors (j, k) in the above stated range. First, $\bar{\xi}_\alpha(j)$ and $\bar{\xi}_\alpha(k)$ are to be read through the curves in Fig. 5. Then, in general cases in which 2- and 3-D differences in various positions of the Munsell solid are under consideration, the predicted difference $\tilde{d}_{jk}$ can be calculated by (9) from $\Delta V = |V_j - V_k|$ and $\Delta\bar{\xi}_\alpha = |\bar{\xi}_\alpha(j) - \bar{\xi}_\alpha(k)|$. If the region encompassing P_j and P_k is limited, $\tilde{d}_{jk}(H,C)$ can be defined by an appropriate set of parameter values given in Table I. The values of $\tilde{d}_{jk}$ tells us that, if the perceptual differences δ_{jk} are converted to the matched V-differences d_{jk}, then d_{jk} will be in the range $\tilde{d}_{jk} \pm$ RMS in about 68% of cases. The root-mean-squares RMS is not necessarily a good index for a single prediction. If necessary, we can estimate the level of possible largest discrepancy from the plots in Fig. 7 or Fig. 8(B).

Prediction (9) based on $\Delta\bar{\xi}_\alpha$ gives smaller RMS (0.338 in terms of matched V-unit) than other predictions. Prediction based on $\hat{d}_{jk}$, Euclidean distance between P_j and P_k in the Munsell solid, gives RMS (0.364). These are larger than RMS when $\hat{d}_{jk}$ are distances between P_j and P_k in the configuration constructed by MDS from the data (d_{jk}). In this case, $\hat{d}_{jk}$ are not predictors, but results obtained from data d_{jk}. Hence, RMS ($0.20 \sim 0.26$ in the matched V-unit) is not an accuracy of prediction, but an index for the reproducibility of MDS. If the accuracy (0.34 matched V-unit) is tolerated, we can conclude that the observer sees an overall color difference as the weighted sum of relevant differences of principal hues and of lightness between two colors.

1. Indow T. Predictions based on Munsell notation. I. Perceptual color differences. Col Res Appl 1999;24:10–18.
2. Indow T. Predictions based on Munsell notation. II. Principal hue components. Col Res Appl 1999;24:19–32.
3. Indow T. Global color metrics and color-appearance systems. Col Res Appl 1980;5:5–12.
4. Indow T. Multidimensional studies of Munsell color solid. Psychol Rev 1988;95:456–470.
5. Jameson D, Hurvich LM. Some quantitative aspects of an opponent-colors theory. I. Chromatic responses and spectral saturation. J Opt Soc Am 1955;45:546–552.
6. Hurvich LH, Jameson D. Some quantitative aspects of an opponent-colors theory. II. Brightness, saturation, and hue in normal and dichromatic vision. J Opt Soc Am 1955;45:602–616.
7. Hurvich LM. Color vision. Sunderland, Massachusetts: Sinauer; 1981.
8. Swedish Standards Institution, SS 019103, Colour atlas, 2nd Ed. Stockholm: SIS; 1989.
9. Tonnquist G. A comparison between symmetrical and equi-spaced hue-circles. Proc Inter Col Meet. Götingen: Musterschmidt Verlag; 1965. pp 376–387.
10. Steen P. Experiments with estimation of perceptive qualitative color attributes. In: Richter M, editor. Color 69. Götingen: Musterschmidt Verlag; 1970. pp 369–376.
11. Hård A, Sivik L, Tonnquist G. NCS, Natural Color system—from concepts to research and applications, Part I. Col Res Appl 1996;21: 180–205.
12. Hård A, Sivik L, Tonnquist G. NCS, Natural Color system—from concepts to research and applications, Part II. Col Res Appl 1996;21: 206–220.
13. Neely G. Magnitude scaling of blackness and chromaticness: A psychophysical evaluation of the NCS in an ecological setting. Rep Dept Psych 792. Stockholm Univ, 1995.
14. NCS: NCS ↔ Munsell. 2nd Ed. Stockholm: Scand Col Inst; 1997.
15. Luce RD. A generalization of a theorem of dimensional analysis. J Math Psych 1964;1:278–284.
16. Krantz DH, Luce RD, Suppes P, Tversky A. Foundation of measurement Vol. 1, Additive and polynomial representations. New York: Academic; 1971.
17. Beckenback E, Bellman R. An introduction to inequalities. New York: Random House; 1961.
18. Indow T, Kanazawa K. Multidimensional mapping of Munsell colors varying in hue, chroma, and value. J Exper Psych 1960;59: 330–336.
19. Indow T, Stevens SS. Scaling of saturation and hue. Percep Psych 1966;1:253–271.
20. Indow T, Ida M. Scaling of dot numerosity. Percep Psych 1977;22: 265–276.
21. Tversky A. Features of similarity. Psych Rev 1977;84:327–352.